

## Article

# Evaluating the Use of Alternative Normalization Approaches on SARS-CoV-2 Concentrations in Wastewater: Experiences from Two Catchments in Northern Sweden

Frida Isaksson <sup>1</sup>, Lian Lundy <sup>1,\*</sup> , Annelie Hedström <sup>1</sup>, Anna J. Székely <sup>2</sup>  and Nahla Mohamed <sup>2</sup>

<sup>1</sup> Department of Civil, Environmental and Natural Resources Engineering, Luleå University of Technology, 971 87 Luleå, Sweden; friisa-4@student.ltu.se (F.I.); annelie.hedstrom@ltu.se (A.H.)

<sup>2</sup> Department of Aquatic Science and Assessment, Swedish University of Agricultural Science, 750 07 Uppsala, Sweden; anna.szekely@slu.se (A.J.S.); nahala.mohamed@slu.se (N.M.)

\* Correspondence: lian.lundy@ltu.se

**Abstract:** The detection of SARS-CoV-2 RNA fragments in feces has paved the way for wastewater-based epidemiology to contribute to COVID-19 mitigation measures, with its use in a public health context still under development. As a way to facilitate data comparison, this paper explores the impact of using alternative normalization approaches (wastewater treatment plant (WWTP) flow, population size estimates (derived using total nitrogen (TN), total phosphorus (TP) and census data) and pepper mild mottle virus (PMMoV)) on the relationship between viral wastewater data and clinical case numbers. Influent wastewater samples were collected at two WWTPs in Luleå, northern Sweden, between January and March 2021. TN and TP were determined upon sample collection, with RNA analysis undertaken on samples after one freeze–thaw cycle. The strength of the correlation between normalization approaches and clinical cases differed between WWTPs ( $r \leq 0.73$  or  $r \geq 0.78$  at the larger WWTP and  $r \leq 0.23$  or  $r \geq 0.43$  at the smaller WWTP), indicating that the use of wastewater as an epidemiological tool is context-dependent. Depending on the normalization approach utilized, time-shifted analyses imply that wastewater data on SARS-CoV-2 RNA pre-dated a rise in clinical cases by 0–2 and 5–8 days, for the larger and smaller WWTPs, respectively. SARS-CoV-2 viral loads normalized to the population or PMMoV better reflect the number of clinical cases when comparing wastewater data between sewer catchments.

**Keywords:** wastewater-based epidemiology; normalization; population estimates; pepper mild mottle virus; clinical cases; infiltration inflow



**Citation:** Isaksson, F.; Lundy, L.; Hedström, A.; Székely, A.J.; Mohamed, N. Evaluating the Use of Alternative Normalization Approaches on SARS-CoV-2 Concentrations in Wastewater: Experiences from Two Catchments in Northern Sweden. *Environments* **2022**, *9*, 39. <https://doi.org/10.3390/environments9030039>

Academic Editors: Vassie Ware, Tiong Gim Aw and Kristen Jellison

Received: 4 February 2022

Accepted: 17 March 2022

Published: 19 March 2022

**Publisher's Note:** MDPI stays neutral with regard to jurisdictional claims in published maps and institutional affiliations.



**Copyright:** © 2022 by the authors. Licensee MDPI, Basel, Switzerland. This article is an open access article distributed under the terms and conditions of the Creative Commons Attribution (CC BY) license (<https://creativecommons.org/licenses/by/4.0/>).

## 1. Introduction

The COVID-19 pandemic, caused by the SARS-CoV-2 virus, has put significant pressure on public health authorities, policy makers and society at large. As a result of its rapid transmission, it has, to-date, resulted in over 290 million confirmed infections worldwide and over 5.4 million deaths [1]. Clinical diagnostics use reverse transcript polymerase chain reaction (RT-PCR) to detect RNA signals of the virus from nasopharyngeal and oropharyngeal swabs as the standard method for clinical testing [2]. The surveillance of virus transmission based on clinical tests performed by healthcare professionals was been insufficient during the formative year of the pandemic due to shortages in staff and consumables, as well as hesitancy to test in some communities [3]. Furthermore, approximately 43–45% of infected individuals can be asymptomatic, with initial data suggesting this may vary by population and by variant [4,5]. As testing focuses on symptomatic cases, the number of cases identified in clinical reports may be an under-representation of the real-world conditions [2].

Despite the fact that COVID-19 is a disease that predominantly affects the respiratory tract, resulting in high prevalence of the virus in respiratory fluids [6], several studies have

reported that SARS-CoV-2 RNA is excreted in feces. While data are still developing, current estimates are that 40.5–51.8% of infected individuals excrete viral RNA fragments in their feces [7,8]. In addressing the identified challenges, considerable interest has focused on the use of wastewater-based epidemiology (WBE). Previously practiced in the monitoring of drug use [9], poliovirus [10] and hepatitis E [11], for example, it is rapidly evolving as a key approach in efforts to monitor the occurrence and spread of the virus in several countries [3,12,13].

The basic premise of WBE is that human excreted substances entering the sewer system can be related to their use by, or exposure to, the contributing population. Thus, by systematic sampling of raw wastewater, a single pooled sample might offer a near real-time, community-wide, snapshot of population health [14]. WBE could serve as a complimentary tool for public health authorities to monitor spatial and temporal trends in virus prevalence, and to detect early warning signs of (re-)emerging outbreaks in a non-invasive and economically effective manner [3,9,12]. Hence, WBE could enhance the public health authorities' preparedness, assisting them in taking necessary precautions to protect public health [2].

However, a variety of factors other than the number of contributing individuals may influence the variability of SARS-CoV-2 concentrations in wastewater. In relation to clinical test data (which typically target symptomatic individuals), wastewater contains inputs from both asymptomatic and symptomatic cases [15]. The fate of SARS-CoV-2 RNA in wastewater and its susceptibility to decay and degradation is observed to be most significantly affected by increasing temperature [16]. Similar behavior has been reported for other enveloped viruses, as well as surrogate viruses which resemble SARS-CoV-2 in their biological and physical properties [14,16–18]. Findings of gamma-irradiated SARS-CoV-2 suggest that the persistence of RNA fragments in raw wastewater, in a range of 4 to 37 °C, is sufficient to produce valid results within the relevant timeframe for wastewater collection and analysis [16].

Whilst clinical data on the shedding of SARS-CoV-2 in feces are limited, data available to date indicate that it does not appear to follow a homogenous pattern amongst clinical cases, with shedding rates ranging between  $10$ – $10^8$  gene copies/g of feces reported [19]. Moreover, the duration of fecal shedding of SARS-CoV-2 has been observed to last for extended periods of time, in many cases outlasting shedding from the respiratory tract [5,6,20,21]. Additionally, due to easy accessibility, studies of fecal shedding of SARS-CoV-2 are conducted primarily on hospitalized symptomatic individuals; this contributes to uncertainties in the patterns of shedding at the beginning of infection and the virus' prevalence in pre- and asymptomatic individuals [2]. However, several studies have detected viral loads in wastewater a few days to weeks prior to clinical diagnostic reports [4,22–25], supporting the supposition that fecal shedding could occur in both pre-symptomatic and asymptomatic phases. Hence, WBE could provide a better indication of the virus' prevalence at a population level, since the sewer system receives concentrations regardless of symptomatic status, supporting its potential as a trend-monitoring tool and early warning system.

Aside from the uncertainty associated with shedding patterns, environmental impacts that may cause dilution in the sewer system and influence WWTP flow (e.g., stormwater and infiltration inflow (I/I)) as well as temporal variations in the number of people contributing to the sewer system (e.g., commuters) increases the difficulty of robust interpretation of the temporal concentration variations [26–28]. Normalization of SARS-CoV-2 wastewater data is one approach to address these deficiencies and promote robust data interpretation that is comparable across samples, as well as WWTPs that can be useful to public health authorities. Wastewater data can be normalized using various parameters, from nutrient concentrations to flow volume. However, the impact of the method chosen on the strength of relationship with clinical case numbers has yet to be thoroughly explored.

Herein, data on the concentration of SARS-CoV-2 in wastewater were normalized to WWTP flow, and the population size estimated based on mass loads of TN and TP, as well as census data and the biomarker PMMoV. Using statistical analyses, the strength of the relationship between the normalization approaches and clinical case data were evaluated. The implications of using alternative normalization methods were identified and recommendations made for future studies.

## 2. Materials and Methods

### 2.1. Sampling Site Description

Wastewater was collected from two WWTPs in Luleå municipality—the Uddebo (UDD) WWTP and the Råneå (RAN) WWTP—at the beginning of 2021. The municipality is situated in the northern part of Sweden along the east coast of Norrbotten county; it has a cold temperate climate [29] and an average precipitation of 600 mm/year, with the highest precipitation rates June–November [30]. UDD is the largest WWTP in Luleå municipality; it is dimensioned for a population equivalent (pe) of 91,000, and has an industrial load equivalent of 15,000 pe, covering the urban catchment area of the Luleå conurbation as well as several larger suburbs [31]. The RAN WWTP is a smaller WWTP, dimensioned for 3800 pe, and has no industrial input. It is located north of Luleå, with a catchment area covering the urban Råneå community [32]. Neither catchment reports major industrial sources of TN or TP, and the use of domestic garbage disposal units is practiced in this area of Sweden. According to census data, 66,600 people are connected to the UDD WWTP and 1971 people are connected to the RAN WWTP, covering 84 and 2.5% of the total population in the municipality, respectively. In excess of the de jure population, the catchment area of UDD WWTP is also influenced by daily commuters and tourists. The majority of the sewage network is made up of separate sewer systems (80–90%); however, infiltration/inflow (I/I) accounts for 47 and 67% of total yearly inflow at the UDD and RAN WWTPs, respectively [31,32].

### 2.2. Wastewater Sampling and Wastewater Quality Characterisation

A total of 32 samples of influent wastewater were collected from UDD and RAN WWTP (from 13 January to 1 March 2021 at the UDD WWTP, and from 1 February to 1 March 2021 at the RAN WWTP). At both locations, 24 h composite samples were collected twice per week with a 72 h composite sample collected over weekends, using a refrigerated flow-proportional autosampler (UDD WWTP) and a refrigerated time-proportional (50 mL every 20 min) autosampler (RAN WWTP). The total composite samples were stirred upon collection, and 3 grab-samples of 100 mL were collected in plastic bottles by WWTP personnel. The samples were stored in a freezer at  $-20\text{ }^{\circ}\text{C}$  until transportation to the laboratory using ice boxes. Average daily flow was recorded on the day of sampling, as was data referring to precipitation and snowmelt. For each composite sample, the concentration (mg/L) of TN and TP were analyzed by the Uddebo accredited laboratory, according to the standard methods SS 02 81 31-1, SM 4500-NO3 B and SS-EN ISO 6878:2005, respectively. Mass loads of TN and TP were calculated for each sampling day by multiplying the concentration with the average daily WWTP flow.

### 2.3. Clinical Case Data

Daily case data of new clinical cases covering the study period were provided by Norrbotten county council in the following format: date of clinical test, date clinical test result was reported, and related postal code for each tested individual [33]. Information on postal code (which did not overlap between the two studied areas) was solely used to allocate clinical data to each WWTP.

While assessing the sufficiency of early warning in this study, the time lag between the day of testing and the day of statistical reports must be kept in mind (average 1–2 days at this time in Luleå municipality). Clinical testing was not significantly hampered by a

lack of resources during this period of the pandemic, and availability of clinical testing was sufficient; therefore, high clinical testing rates may be presumed.

#### 2.4. SARS-CoV-2 Concentration and RNA Extraction

Viral total nucleic acid (TNA) was concentrated from duplicate wastewater samples for each sample using a Maxwell RSC Environmental TNA Kit, AX9560 (Promega) according to the manufacturer's protocol. This method has an excellent ability to eliminate RT-qPCR inhibitors. Briefly, protease solution was added to 40 mL of wastewater sample and incubated for 30 min at room temperature. Following the digestion step, solids were removed by centrifugation and nucleic acids were concentrated by a column-based system. The 0.5 mL of nucleic acids eluted from the column were further purified using the provided Maxwell cartridge and the PureFood GMO and Authentication program of the Maxwell RSC instrument (Promega). In the final step, the instrument eluted the nucleic acids in 80  $\mu$ L of nuclease-free water [34]. In-house assessment of the recovery efficiency of the method using Bovine Coronavirus (BCoV) were in line with the efficiency and consistency expected according to the manufacturer ( $23 \pm 3\%$ ).

#### 2.5. RT-qPCR

The extracted TNA was used to perform one-step RT-qPCR quantification of the genetic material of SARS-CoV-2 and PMMoV, separately. SARS-CoV-2 was quantified using the U.S. Center for Disease Control primer sets [35], while PMMoV was quantified using the primer sets described in Zhang et al. (2006) [36]. All qPCR quantifications were performed according to the MIQE guidelines [37], and only analyses with PCR amplification efficiencies between 90 and 120% were accepted. A serial dilution of CDC RUO 2019-nCoV\_N Positive Plasmid Control (IDT DNA, Cat # 10006625) and a manufactured plasmid containing the appropriate target sequence (IDT DNA, Custom MiniGene 25–500 bp) were used to generate standard curves using linear regression of the relationship between the Cq values and copy numbers. Samples were analyzed in triplicate using the Reliance One-Step Multiplex Supermix kit (BioRad), following the manufacturer's protocol and in the presence of 1 mg/mL BSA (ThermoFisher). Each 20  $\mu$ L reaction contained 5  $\mu$ L template RNA or nuclease free water for the non-template controls (NTCs). The reactions were run according to the following thermal profile using a CFX96 Touch Real-time PCT Detection system (BioRad): 50  $^{\circ}$ C for 30 min and 95  $^{\circ}$ C for 5 min; followed by 45 cycles of 95  $^{\circ}$ C for 15 s and 60  $^{\circ}$ C for 30 s for N1; and 58  $^{\circ}$ C for 30 s for PMMoV. Samples were reported positive only for Ct values < 40 and when the RT-qPCR assay triplicates of each wastewater sample had a Ct standard deviation < 0.45. If removing outliers did not improve the standard deviation, RT-qPCR triplicates with Ct standard deviation > 0.45 were disregarded. The concentration of SARS-CoV-2 and PMMoV genomes in each sample, C (copies/mL), was calculated using Equation (1).

$$C = N / (V_{\text{RT-qPCR}} \times (V_{\text{sample}} / V_{\text{extracted}})) \quad (1)$$

where N (copies/reaction) is the gene copies detected in each RT-qPCR reaction;  $V_{\text{RT-qPCR}}$  (mL) is the volume of TNA used for RT-qPCR;  $V_{\text{sample}}$  (mL) is the wastewater sample volume initially used for the concentration step; and  $V_{\text{extracted}}$  (mL) is the total volume of nucleic acid extracted using the Maxwell RSC instrument (Promega).

#### 2.6. Estimations of Population Size and Normalization of SARS-CoV-2 Concentrations

The daily viral load, VL (copies/d), for both SARS-CoV-2 and PMMoV was calculated by normalizing C to the average daily WWTP flow, Q (L/d) (Equation (2)).

$$VL = C \times Q \times 10^3 \quad (2)$$

Mass loads of TN and TP in wastewater,  $M_{\text{TN/TP}}$  (g/d), were utilized to estimate the size of the contributing population (P) on each day of sample collection (see Equation (3)). In this study, four values of the domestic contribution of TN and TP sourced from the

literature,  $m_{\text{TN/TP}}$  (g/p/d), were used, with values ranging from 12.5–14.0 g/p/d for TN and 1.2–2.1 g/p/d for TP (see Tables S1 and S2 for specific values [38–41]).

$$P = M_{\text{TN/TP}} / m_{\text{TN/TP}} \quad (3)$$

Subsequently, divisions of VL by P were applied for population normalization of the viral loads, resulting in an expression of copies/p/d. Normalization of SARS-CoV-2 RNA using the biomarker PMMoV was undertaken by dividing the VL of SARS-CoV-2 RNA (N) by the VL of PMMoV for each sampling day.

### 2.7. Statistical Analyses

Intraday variations of the different approaches of estimating the population size, as well as the variability between weekday and weekend data sets, were measured as relative standard deviation (RSD) and expressed as a percentage (%) of variation (Equation (4)).

$$\text{RSD} = (\text{SD} / \bar{x}) \times 100 \quad (4)$$

where SD is the standard deviation and  $\bar{x}$  is the mean value of the data. A Pearson correlation test was used to assess the type of relationship between the different normalization approaches of SARS-CoV-2 in wastewater and epidemiological data. The Pearson correlation coefficient for each normalization approach and the associated 7-day rolling average of clinical cases per 100,000 inh. were compared across the two WWTPs and between normalization approaches. All normalization approaches were also subjected to a time-shifted correlation. A period of 1 to 10 days was used to offset the association between each normalization procedure and clinical cases. The difference in Ct values between sample replicates of SARS-CoV-2 and PMMoV was analyzed as a process efficiency measurement. A Ct difference  $> \pm 0.90$  was utilized as an indication of a low level of reproducibility in analytical procedures between sample replicates. All statistical analyses and data processing were performed in MS Excel.

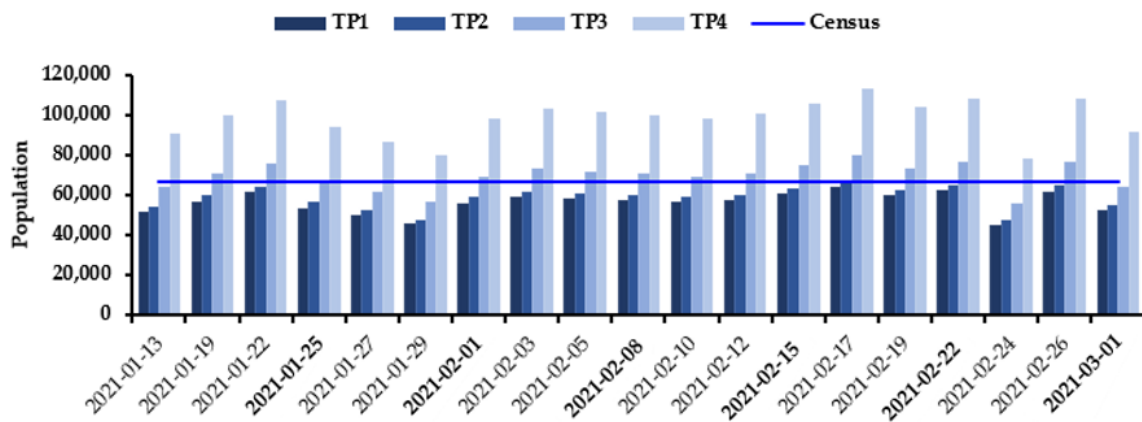
## 3. Results and Discussion

### 3.1. Estimations of Population Size

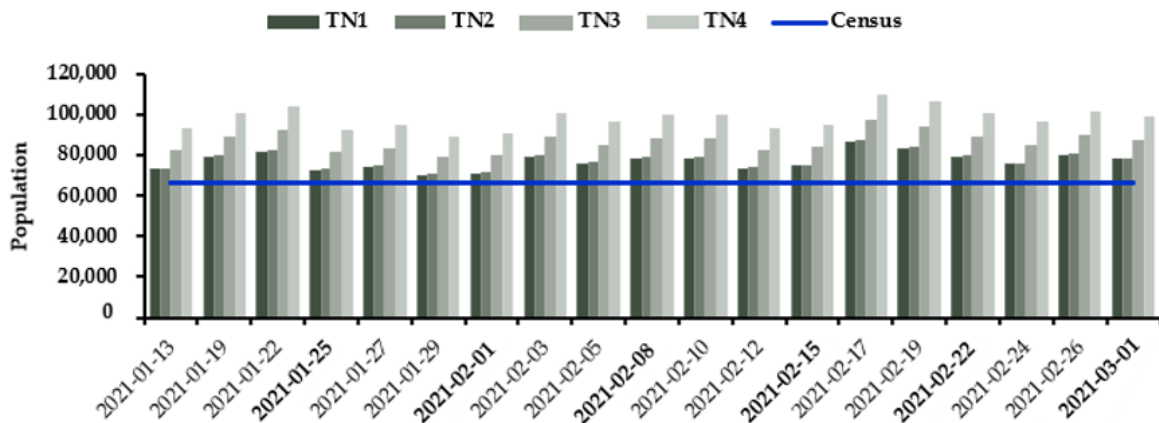
In the context of WBE, several studies have attempted to estimate population size using different human markers found in wastewater, since census data do not consider diurnal dynamics of the population size [26,38,42]. In Sweden, WWTPs routinely analyze TN and TP; therefore, using reported literature values of the domestic input per person of these parameters, it provides an easy and effective way to investigate temporal population variations. The selected values (see Supplementary Materials Tables S1 and S2) were applied in the study as they reflect the range of values typically used in Sweden [38–41]. The population size estimates vary significantly between TN and TP estimations and between the literature values used for each parameter—from 44,822 to 112,702 at the UDD WWTP (Figure 1a,b), and from 984 to 4291 at the RAN WWTP (Figure 2a,b).

At the UDD WWTP, the average deviation for all the population estimations from census data is 6.1% for the TP estimated population and 28% for the TN estimated population. For the RAN WWTP, similar results can be seen, wherein the average deviation from census data is −2.8% for the TP estimated population and 8.5% for the TN estimated population. This suggests that the TP estimated population yields a result that is close to census data, whereas TN generally overestimates the population size compared to the census data. However, intraday variations, measured as relative standard deviation (RSD), between the four literature values utilized for the domestic contribution of each parameter to the sewer system, are lower for TN (RSD 10%) than for TP (RSD 24%). Hence, even though the average deviation from census data is lower for TP-derived estimations, the extreme values of population estimations during the sampling period at both WWTPs are represented by those calculated based on TP mass loads. Given that the data were collected during a

time when many people were working from home (and therefore presented limited daily variations), the use of TN-derived population estimates is considered to be more robust.

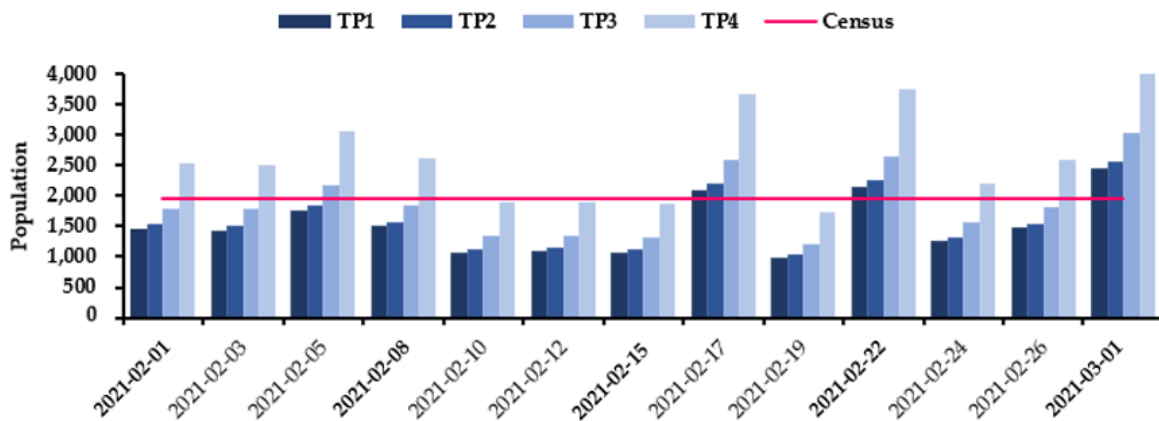


(a)



(b)

**Figure 1.** Overview of census and estimated population size at UDD WWTP on the identified sampling dates, wherein population size is estimated using four TP excretion rates (a) and four TN excretion rates (b) (note: dates in bold indicate 72 h (weekend) samples).



(a)

**Figure 2.** Cont.

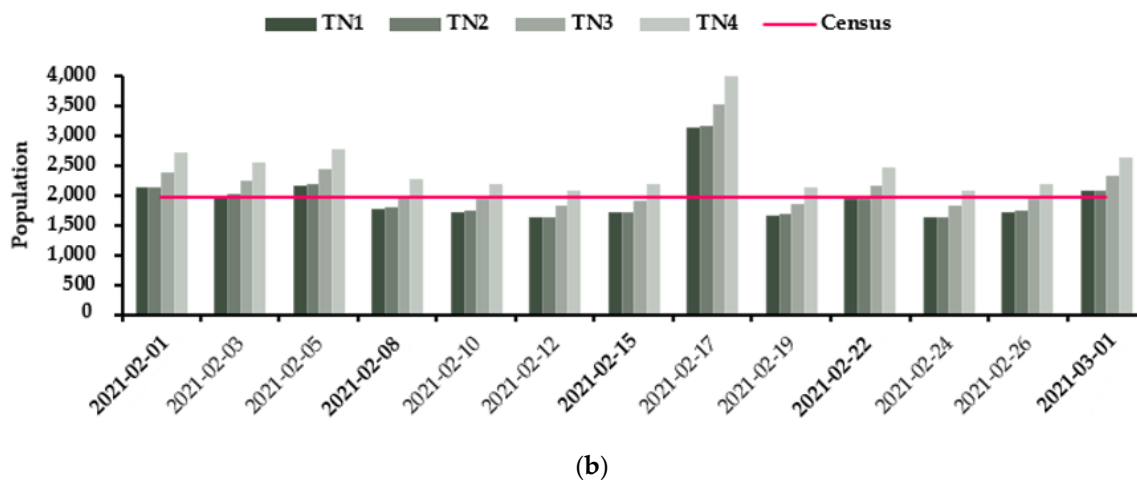


**Figure 2.** Overview of census and estimated population size at RAN WWTP on the identified sampling dates, wherein population size is estimated using four TP excretion rates (a) and four TN excretion rates (b) (note: dates in bold indicate 72 h (weekend) samples).

When comparing weekdays and weekend data sets, weekends TN-derived population estimates exhibit less variability (RSD 4.1% at the UDD WWTP and 8.3% at the RAN WWTP) than weekdays (RSD 5.7% at the UDD WWTP and 24.5% at the RAN WWTP) (see Supplementary Materials Tables S3 and S4). At the UDD WWTP, the same result can be seen for the TP estimated population (RSD 10.6% on weekdays and RSD 6.1% on weekends). However, this pattern does not apply to TP population estimations at the RAN WWTP (RSD 25.4% on weekdays and 29.1% on weekends). These patterns could imply that the population size is more constant on weekends based on the TN mass loads. However, this result could be a function of the fact that contributions from industrial activities are reduced on weekends at the UDD WWTP (industrial input equal to 15,000 pe) [42,43], and further work is required to enable the influences and inter-relationships between these two factors to be resolved.

During the pandemic in Sweden, lockdowns have not been applied; instead, more modest restrictions and recommendations have been implemented, encouraging people to be more restrictive in their travel and commuting patterns, as well as encouraging people to work from home. Even though minimal diurnal population variations were expected during this time, a constant state, as might be expected with lockdowns, cannot be assumed. Therefore, the temporal trend observed for estimations of the population size might be an indicator of fewer commuters during the weekend; this suggests that the estimated population size based on TP and TN might be more adequate than population size based on census data.

### 3.2. Detection and Quantification of SARS-CoV-2 RNA in Wastewater Samples

Out of the 32 wastewater samples collected, all UDD WWTP samples ( $n = 19$ ) and 77% of RAN WWTP samples ( $n = 13$ ) were RT-qPCR positive for the N1 gene (all RT-qPCR NTCs were negative) (see Supplementary Materials Tables S5 and S6). All positive samples had mean Ct values below 35, with ranges of 29.2–34.5 and 29.9–34.8 at the UDD and RAN WWTPs, respectively, with the SD of RT-qPCR triplicates being  $<0.45$ . In the absence of measurements performed on fresh samples, the exact impact of freezing could not be evaluated. However, the measured SARS-CoV-2 concentrations were in the range of 10.7–144.9 copies N1/mL at the UDD WWTP and 2.9–169.1 copies N1/mL at the RAN WWTP (see Supplementary Materials Tables S5 and S6), indicating that the applied method was robust to one freeze–thaw cycle. A comparison of the difference in Ct values between replicates for each sampling date demonstrated sufficient concordance for the majority of the analyzed samples (see Supplementary Materials Tables S5 and S6), with the

average Ct difference for N1 being 0.49 at the UDD WWTP and 0.47 at the RAN WWTP. The result demonstrates sufficient concordance, indicating strong to very strong levels of reproducibility in the analytical procedures between sample replicates.

### 3.3. Detection and Quantification of PMMoV RNA in Wastewater Samples

Among the samples collected in this study, they all detected strong signals of PMMoV in the RT-qPCR, with mean Ct values in the range of 22.3–25.0 at the UDD WWTP and 21.9–24.6 at the RAN WWTP. On a few sampling occasions, the SD of the Ct values from RT-qPCR duplicates from the initial analysis exceeded 0.45 (see Supplementary Materials Tables S7 and S8 for specific days) and their concentrations were lower than the expected, indicating analytical errors in the first RT-qPCR run. Hence, RT-qPCR was repeated on the specific samples. PMMoV concentrations were in the range of  $2.4 \times 10^4$ – $1.5 \times 10^5$  copies/mL at the UDD WWTP and  $3.1 \times 10^4$ – $2.0 \times 10^5$  copies/mL at the RAN WWTP (see Supplementary Materials Tables S7 and S8). At both the UDD WWTP and the RAN WWTP, the average Ct difference for PMMoV between duplicates for each sampling date was 0.56 (see Supplementary Materials Tables S7 and S8 for specific values). Samples with a Ct difference > 0.90 included replicates that were re-analyzed. However, the result demonstrates sufficient concordance, indicating strong levels of reproducibility in the analytical procedures between sample replicates.

### 3.4. Different Normalization Approaches for SARS-CoV-2 in Wastewater and Correlation to Clinical Case Data

The sampling period covers an initial period of low clinical case numbers (282 and 0 clinical cases per 100,000 inhabitants (inh.) per week at the UDD and RAN WWTPs, respectively), followed by an increase to a maximum of 787 clinical cases/100,000 inh. at the UDD WWTP and 913 clinical cases/100,000 inh. at the RAN WWTP per week (see Supplementary Materials Figure S1a,b).

At the UDD WWTP, the 7-day rolling average of clinical cases has a strong correlation initially (daily offset 0, i.e., no time shift) to unnormalized data, as well as all normalization approaches (Tables 1 and 2). For un-normalized data, as well as SARS-CoV-2 normalized to WWTP flow and PMMoV, the correlation peaks at a two-day time-shift. However, out of all the approaches, viral loads normalized to the TP estimated population had the strongest correlation to clinical cases without any time shift. In contrast, the approach of normalizing viral loads using PMMoV reveals the weakest correlation to clinical cases at its maximum at two days offset; however, the difference in the strength of the correlations between the different approaches applied was minimal (0.73 as the lowest and 0.78 as the highest). At the RAN WWTP, the Pearson correlation coefficient initially (daily offset 0) shows a weak-to-moderate correlation to clinical cases in all the normalization approaches, which gradually increases to a very strong correlation in the time-shifted analyses. In contrast to the results obtained at the UDD WWTP, the approach of normalizing viral loads using the TP estimated population indicates the weakest correlation to clinical cases at the RAN WWTP.

**Table 1.** Time-shifted analyses of the Pearson correlation coefficients (r) at UDD WWTP between un-normalized as well as normalized SARS-CoV-2, and the 7-day rolling averages of clinical cases offset over a time period of 1–10 days (where 0 refers to the wastewater sample collection date).

	Daily Offset										
	0	1	2	3	4	5	6	7	8	9	10
Un-normalized	0.764	0.771	0.776	0.771	0.768	0.766	0.739	0.707	0.632	0.572	0.508
Normalized to WWTP flow	0.763	0.766	0.768	0.761	0.755	0.752	0.723	0.690	0.613	0.553	0.487
Normalized to TN estimated population	0.752	0.750	0.749	0.741	0.735	0.736	0.702	0.667	0.592	0.530	0.465
Normalized to TP estimated population	0.776	0.759	0.748	0.731	0.725	0.724	0.679	0.640	0.562	0.495	0.432
Normalized to PMMoV viral loads	0.734	0.735	0.748	0.746	0.695	0.667	0.652	0.615	0.549	0.507	0.447

Key: shading indicates the highest level of correlation per parameter.

**Table 2.** Time-shifted analyses of the Pearson correlation coefficients ( $r$ ) at RAN WWTP between un-normalized as well as normalized SARS-CoV-2, and the 7-day rolling averages of clinical cases offset over a time period of 1–10 days (where 0 refers to the wastewater sample collection date).

	Daily Offset										
	0	1	2	3	4	5	6	7	8	9	10
Un-normalized	0.408	0.591	0.629	0.732	0.781	0.854	0.878	0.862	0.860	0.851	0.780
Normalized to WWTP flow	0.418	0.586	0.627	0.726	0.758	0.835	0.846	0.826	0.828	0.815	0.753
Normalized to TN estimated population	0.421	0.592	0.623	0.695	0.737	0.824	0.784	0.774	0.746	0.733	0.674
Normalized to TP estimated population	0.230	0.397	0.434	0.499	0.596	0.691	0.704	0.686	0.754	0.731	0.746
Normalized to PMMoV viral loads	0.435	0.649	0.653	0.711	0.841	0.841	0.888	0.875	0.766	0.773	0.636

Key: shading indicates the highest level of correlation per parameter.

Depending on the normalization approach used, time-shifted analyses of the Pearson correlation coefficient suggest that wastewater data of SARS-CoV-2 RNA pre-date rises in clinical cases by 0–2 days at the UDD WWTP and 5–8 days at the RAN WWTP (Tables 1 and 2). Whilst the specific reasons for the difference in the time-shift duration between the two sites are not clear, potential factors could include differences in people’s willingness to be tested, age profiles, and sewer system travel times. Based on this study, this could be an indication that WBE has a stronger predictive value for smaller WWTPs. However, further studies are needed to completely comprehend the changes in WBE predictability between different sized WWTPs.

#### 3.4.1. SARS-CoV-2 WWTP Flow Normalization

To account for variations in flow between days due to factors such as precipitation, snowmelt or groundwater inflow, normalization of SARS-CoV-2 concentrations using the average daily WWTP flow was applied, resulting in an expression of the N1 gene in viral loads (N1 copies/d). The volume of inflow slightly decreased over the sampling period at both WWTPs. The flow was, on average,  $2.57 \times 10^4 \pm 1.59 \times 10^3 \text{ m}^3/\text{d}$  at the UDD WWTP and  $6.79 \times 10^2 \pm 7.07 \times 10^1 \text{ m}^3/\text{d}$  at the RAN WWTP (see Supplementary Materials Figure S2a,b); this modest change in flow explains the limited (if any) effect on the strength of correlation between flow-normalized and un-normalized data (Tables 1 and 2). Throughout the sampling period, temperatures above zero were not recorded until the last few days of the study period. Hence, most of the precipitation fell as snow, suggesting that stormwater had no impact on the sewage system’s flow volumes during the sampling campaign. The limited reduction in inflow volumes observed over time is also linked to the reported cold weather conditions whereby a lack of stormwater recharge of groundwater leads to falling groundwater levels, which, in turn, reduces levels of groundwater infiltration to piped systems.

Regardless of the minimal influence on the correlation that this normalization approach has on the data set, normalization to flow is essential to account for systematic variations within a WWTP. If samples had been collected during this region’s snow melt season, flow rates would have been substantially higher, and large variations between days could have been expected, resulting in greater variations in the data. Hence, the detected signals of SARS-CoV-2 RNA expressed as raw concentrations are likely to be insufficient to provide information about viral occurrence and behavior during all seasons; this is because an increase could be caused by a higher number of infected individuals, or a function of dry weather and, thus, less dilution from stormwater and/or groundwater.

The results of the time-shifted correlation coefficients (Tables 1 and 2 and Figure 3a,b) indicate an increase in viral load before clinical cases begin to rise. This further suggests that SARS-CoV-2 normalized to WWTP flow could have predicted an increase in clinical cases ahead of time. However, while clinical cases continue to rise in the subsequent time period, the first increase in SARS-CoV-2 in wastewater at the UDD WWTP is followed by a decline (between 8 and 10 February) before rising again. In the context of public health, this could lead to confusion and the misconception that viral transmission is decreasing.

Therefore, the influence of additional factors and interactions on virus behavior in-pipe needs further research. However, it is important to note that the magnitude of the viral loads was substantially higher at the UDD WWTP compared to that at the RAN WWTP (see secondary Y axes in Figure 3a,b).

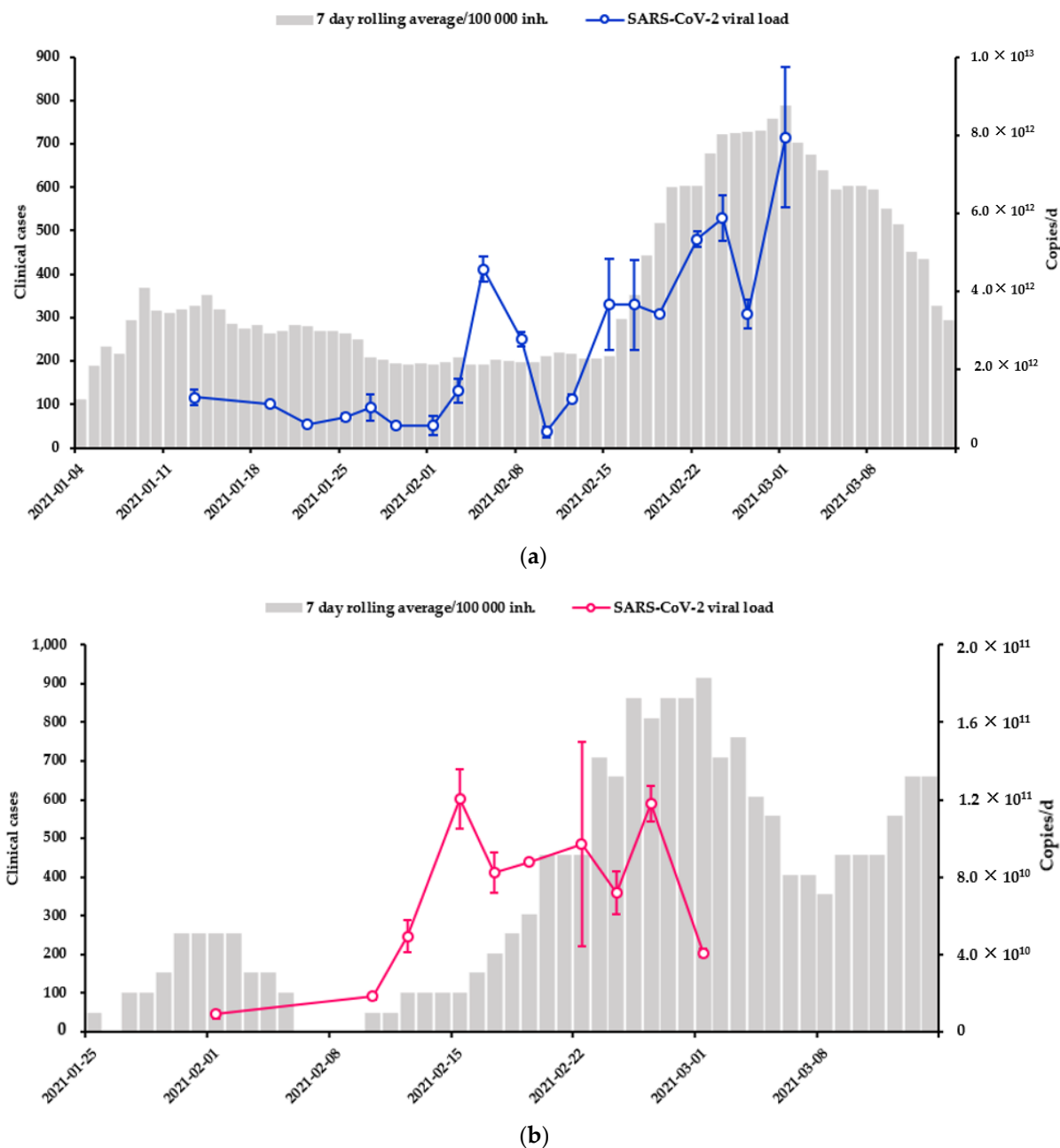


**Figure 3.** Longitudinal data of flow-normalized SARS-CoV-2 viral loads together with clinical cases, presented as 7 day rolling average per 100,000 inh. (based on day of testing) at: (a) UDD WWTP and (b) RAN WWTP (note: the date indicates the first Monday of each week and error bars depict the standard deviation of sampling date replicates).

### 3.4.2. SARS-CoV-2 Population and PMMoV Normalization

Even though population size cannot be predicted with a high level of confidence, the goal of assessing an estimated population based on different estimations is to better reflect the influence that population changes have on the detected signals of SARS-CoV-2 in wastewater [12,44,45], and thus, the implications for public health decision-makers. The

estimations of population size described in Section 3.1 were applied to further normalize the viral loads (Section 3.4.1) in order to include the effect of population dynamics on SARS-CoV-2 wastewater data (Figure 4a,b). SARS-CoV-2 normalized to census data is the same as viral load, since census data are constant. However, for comparison of population normalization procedures, this is included in Figure 4a,b.

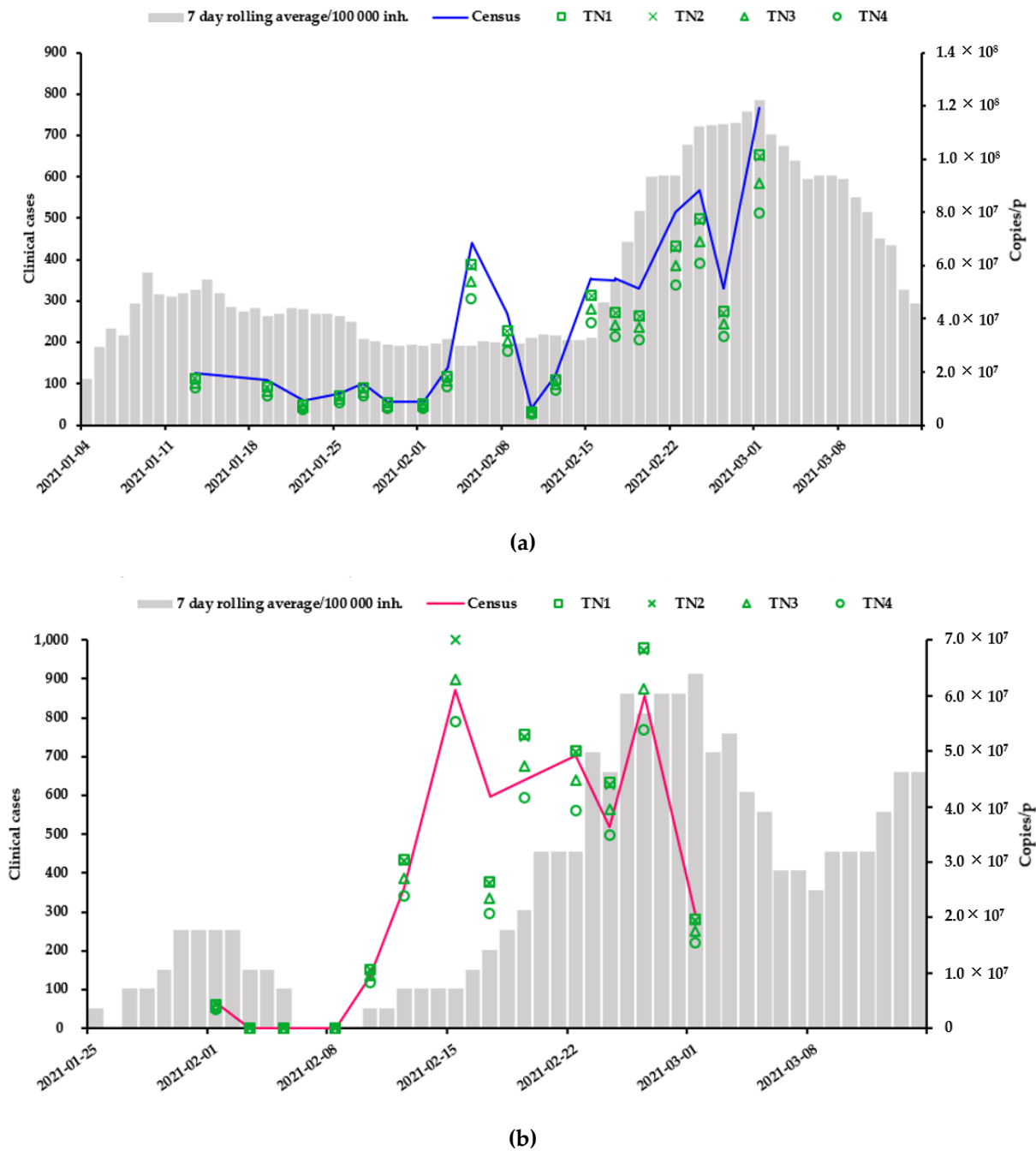
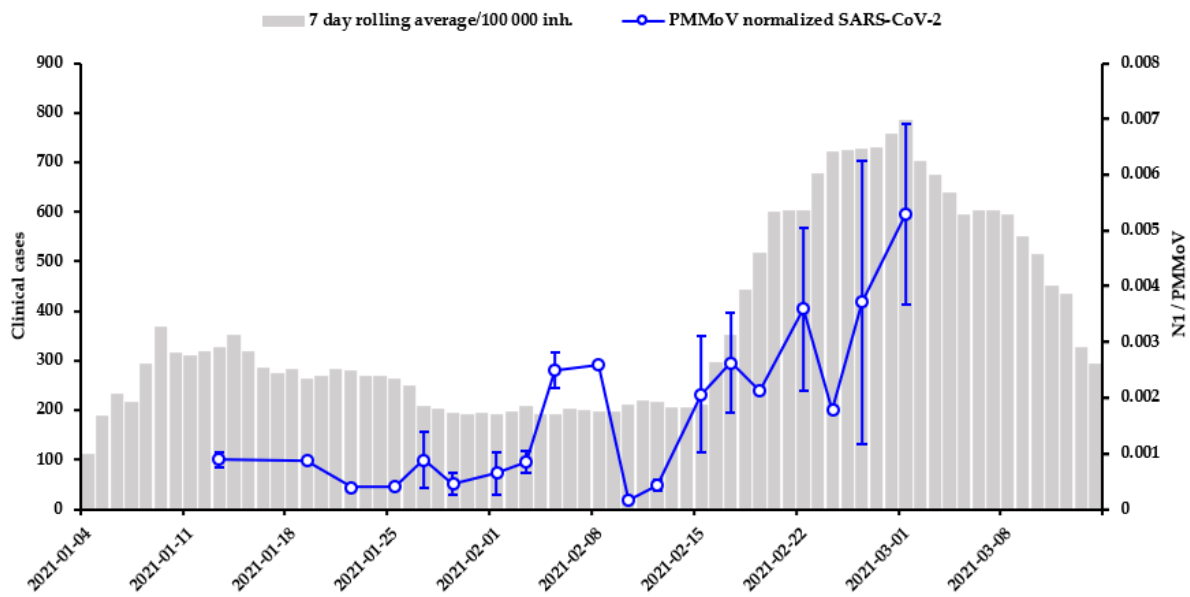


**Figure 4.** Longitudinal data of SARS-CoV-2 viral loads (copies/d) normalized to census population (census) and TN estimated population size (TN1-TN4 benchmarked with daily new clinical cases per 100,000 inh. based on day of testing at (a) UDD WWTP and (b) RAN WWTP (note: the date identified is the first Monday of every week).

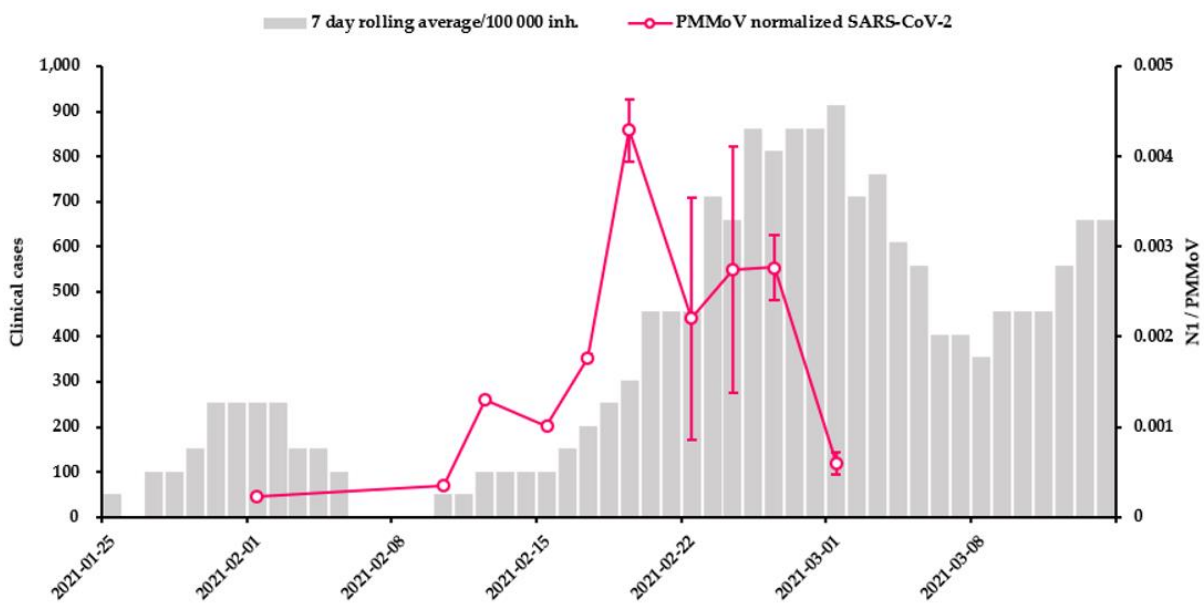
When comparing the magnitude of population-normalized SARS-CoV-2 viral loads, it can be seen that the difference between data normalized using TN population estimations and census data fall within the same order of magnitude at both WWTPs (Figure 4a,b). A similar trend is seen for viral wastewater data normalized to TP estimated population size (see Supplementary Materials Figure S3a,b). Previous studies estimating population size based on other parameters, to infer temporal changes in illicit drug use, have reported similar results [46]. Hence, despite the fact that TN and TP estimated population size deviates (to differing degrees) from the census data over the sampling period, the relationship between the normalized viral loads and clinical case-numbers were relatively insensitive to whether census population or population size estimates were used. However, the data also indicate the potential limitations of using viral data normalized only to flow in a public health context; the presentation of flow-normalized loads, independent of case numbers (see secondary Y axes in Figure 3a,b), may suggest that the virus was more prevalent in the catchment area of the UDD WWTP compared to the RAN WWTP, a picture which changed when data were further normalized for population size.

PMMoV is a plant virus that is found in human feces as a result of eating peppers and pepper-processed foods. It is the most abundant RNA virus found in healthy individuals and it has been discovered to be highly stable in wastewater. PMMoV is also shed in large quantities—up to  $10^9$  gene copies/g feces—and is often utilized as a marker of wastewater pollution in environmental waters [36, 47–48]. As a result, interest in utilizing PMMoV as an internal reference virus to normalize SARS-CoV-2 in wastewater has increased [27]. Theoretically, this normalization approach would account for flow variations, and loss due to storage and sample processing, as well as population dynamics (i.e., these factors would affect the concentration of both PMMoV and SARS-CoV-2) [49]. However, the effects of freezing and thawing may have varying degrees of impact on the viruses, and further research to support the development of a more complete understanding of the impact of freeze–thaw cycles is required. Several studies have reported that PMMoV shows minimal geographic and seasonal variation [44,45,47]. However, PMMoV concentrations originate from the consumption of PMMoV-infected plants which may vary between regions due to social and cultural variations influencing food habits.

When examining the effect of PMMoV normalization on the longitudinal data sets, a temporal trend comparable to SARS-CoV-2 normalized to WWTP flow and population can be seen at both WWTPs (Figure 5a,b). When compared to flow-normalized SARS-CoV-2, the magnitude of the normalized data using this approach more accurately reflects the number of clinical cases/100,000 inh. at the two WWTPs in a manner similar to population normalization. Comparing viral loads normalized to population or PMMoV with clinical cases indicates that the temporal variations follow the same pattern as the viral loads (Figure 3a,b). Moreover, after the first peak (between 8 and 10 February) in normalized SARS-CoV-2 data at the UDD WWTP, both the population- and PMMoV-normalized data sets showed a decline in normalized SARS-CoV-2 data in the same way as WWTP flow normalized data. The normalized data could decrease if the population of the area suddenly increased while infection rates remained unchanged. However, no such relationship could be found in this study based on population estimates at the time (Figure 1a,b).



(a)



(b)

**Figure 5.** Longitudinal data of PMMoV-normalized SARS-CoV-2 (copies/copies PMMoV) benchmarked with daily new clinical cases based on day of testing at: (a) UDD WWTP and (b) RAN WWTP. The datemark display is held on the first Monday of every new week. Error bars depict the standard deviation of sampling date replicates.

### 3.5. Future Research Recommendations

This study involved the use of frozen samples, stored for 18 weeks at  $-20\text{ }^{\circ}\text{C}$ , and exposed to a single thaw cycle before RNA concentration and extraction. Whilst some studies have reported a negative impact of the freeze–thaw cycle on signal strength [48], in-house evaluation of the impact of freezing indicated that the freeze–thaw process did not significantly affect the recovery of N1 ( $p = 0.47$  and  $p = 0.49$ ). The recovery of PMMOV was higher in the frozen samples (potentially due to the release from solid materials), and further research is required to evaluate the impact of freeze–thaw cycles on PMMoV behavior.

Moreover, the samples used in this study were obtained during cold winter conditions (with minimal changes in flow reported over the sampling campaign), which are ideal circumstances for SARS-CoV-2 detection in wastewater [14]. However, the specific effect of dilution and temperature changes on SARS-CoV-2 in wastewater should be investigated further. In addition, the results indicate that a time shift between wastewater data and clinical case numbers, as well as a greater understanding of the factors contributing to the time shift (e.g., in-pipe behavior and understanding of whether time shifts are consistent on a catchment basis), will increase the utility of the approach as a public health tool. Another issue that should be further investigated is what detection limit should cause concern in public health officials. The study showed that the surveillance of SARS-CoV-2 viral loads normalized to population can be sufficient for detecting temporal changes in viral occurrence, although it may be difficult to interpret the data if levels are already high.

Population normalization of viral loads might become more crucial as society opens up and the population deviates further from census data, particularly in places with exceptionally high diurnal variations, such as commuter and tourist-influenced cities. Population dynamics may have a different impact on SARS-CoV-2 wastewater data as more people are vaccinated, resulting in decreased virus prevalence in communities. Therefore, it would be interesting to explore how the population normalization of viral loads, using an estimated de facto population on a bigger population with more variable population dynamics, would compare to those normalized to census data as clinical cases decrease.

#### 4. Conclusions

This study explored the implications of the use of alternative normalization approaches on SARS-CoV-2 in wastewater using WWTP flow, with population size estimated based on mass loads of TN and TP, as well as the biomarker PMMoV. This case study identified the following:

Time-shifted analyses of the Pearson correlation coefficient suggest that wastewater data of SARS-CoV-2 RNA pre-date rises in clinical cases by 0–2 days at the larger WWTP (UDD) and 5–8 days at the smaller WWTP (RAN), depending on the normalization approach utilized. Additionally, a strong correlation for all values was found across both WWTPs. However, whilst none of the normalizations approaches substantially improved the strength of the relationship between clinical case numbers and SARS-CoV-2 in wastewater normalization, they are important in terms of understanding trends in data and supporting comparisons between sites.

The magnitude of SARS-CoV-2 viral loads normalized to estimated population or PMMoV better reflect the number of clinical cases compared to those solely normalized to WWTP flow. Hence, these approaches could provide more robust information for comparing viral transmission between different areas using SARS-CoV-2 wastewater data.

As a case study, further research with larger data sets, generated over a longer time period, is needed to support development of a more complete understanding of the impact of normalization approaches under, for example, changing climatic conditions.

**Supplementary Materials:** The following supporting information can be downloaded at: <https://www.mdpi.com/article/10.3390/environments9030039/s1>, Figure S1: Daily new clinical cases per 100,000 inh. over the sampling period in the catchment area of: (a) UDD WWTP and (b) RAN WWTP. The datemark display is held on the first Monday of every new week; Figure S2: Average daily WWTP flow over the sampling period at: (a) UDD WWTP and (b) RAN WWTP; Figure S3: Longitudinal data of SARS-CoV-2 viral loads normalized to census population (census) and TP estimated population size (TP1-TP5) benchmarked with daily new clinical cases per 100,000 inh. based on day of testing at: (a) UDD WWTP and (b) RAN WWTP. The datemark display is held on the first Monday of every new week; Table S1: Content of total nitrogen (TN) in domestic wastewater (expressed as g/p/d) based on literature values of excretion in faeces and urine, as well as contribution from greywater; Table S2: Content of total phosphorous (TP) in domestic wastewater (expressed as g/p/d) based on literature values of excretion in faeces and urine, as well as contribution from greywater; Table S3: Weekend and weekday average TP and TN population estimations and corresponding

relative standard deviation (RSD) at UDD WWTP; Table S4: Weekend and weekday average TP and TN population estimations and corresponding relative standard deviation (RSD) at RAN WWTP; Table S5: UDD WWTP Ct values and calculated Ct difference between replicates, as well as calculated concentrations in each sample. Each replicate is based on an average value from RT-qPCR triplicates targeting the N1 gene of SARS-CoV-2; Table S6: RAN WWTP Ct values and calculated Ct difference between replicates, as well as calculated concentrations in each sample. Each replicate is based on an average value from RT-qPCR triplicates targeting the N1 gene of SARS-CoV-2; Table S7: UDD WWTP Ct values from RT-qPCR of PMMoV and calculated Ct difference, as well as calculated concentrations in each sample replicate. Each replicate is based on an average value from RT-qPCR duplicates; Table S8: RAN WWTP Ct values from RT-qPCR of PMMoV and calculated Ct difference, as well as calculated concentrations in each sample replicate. Each replicate is based on an average value from RT-qPCR duplicates.

**Author Contributions:** Conceptualization, F.I., L.L., A.H. and A.J.S.; methodology, L.L., A.H., A.J.S. and N.M.; validation, F.I., A.J.S. and N.M.; formal analysis F.I. and N.M.; investigation F.I., A.J.S., L.L. and A.H.; resources, L.L., A.H., A.J.S. and N.M.; data curation F.I.; writing—original draft preparation, F.I., L.L. and A.H.; writing—review and editing, F.I., L.L., A.H., A.J.S. and N.M.; visualization, F.I.; supervision, L.L., A.H., A.J.S. and N.M.; project administration, A.H.; funding acquisition, A.J.S., L.L. and A.H. All authors have read and agreed to the published version of the manuscript.

**Funding:** This research was funded by VINNOVA (Swedish Governmental Agency for Innovation Systems), DRIZZLE—Centre for Stormwater Management (Grant no. 2016-05176), and the Knut and Alice Wallenberg Foundation’s grant through SciLifeLab for research on COVID-19 (KAW 2020.0241, V-2020-0699).

**Institutional Review Board Statement:** Not applicable.

**Informed Consent Statement:** Not applicable.

**Data Availability Statement:** Data are contained within the article or supplementary material.

**Acknowledgments:** The authors acknowledge the Luleå Municipality wastewater treatment plant for contributing to the collection of samples and wastewater analyses, as well as Norrbotten county council for contributing to the clinical case data. We also gratefully acknowledge the technical expertise provided by the Stormwater&Sewers network.

**Conflicts of Interest:** The authors declare no conflict of interest. The funders had no role in the design of the study; in the collection, analyses, or interpretation of data; in the writing of the manuscript; or in the decision to publish the results.

## References

1. WHO Coronavirus (COVID-19) Dashboard. Available online: <https://covid19.who.int> (accessed on 8 January 2022).
2. Zhu, Y.; Oishi, W.; Maruo, C.; Saito, M.; Chen, R.; Kitajima, M.; Sano, D. Early warning of COVID-19 via wastewater-based epidemiology: Potential and bottlenecks. *Sci. Total Environ.* **2021**, *767*, 145124. [[CrossRef](#)] [[PubMed](#)]
3. Michael-Kordatou, I.; Karaolia, P.; Fatta-Kassinos, D. Sewage analysis as a tool for the COVID-19 pandemic response and management: The urgent need for optimised protocols for SARS-CoV-2 detection and quantification. *J. Environ. Chem. Eng.* **2020**, *8*, 104306. [[CrossRef](#)] [[PubMed](#)]
4. Ahmed, W.; Tschärke, B.; Bertsch, P.M.; Bibby, K.; Bivins, A.; Choi, P.; Clarke, L.; Dwyer, J.; Edson, J.; Nguyen, T.; et al. SARS-CoV-2 RNA monitoring in wastewater as a potential early warning system for COVID-19 transmission in the community: A temporal case study. *Sci. Total Environ.* **2021**, *761*, 144216. [[CrossRef](#)] [[PubMed](#)]
5. Walsh, K.A.; Jordan, K.; Clyne, B.; Rohde, D.; Drummond, L.; Byrne, P.; Ahern, S.; Carty, P.G.; O’Brian, K.K.; O’Murchu, E.; et al. SARS-CoV-2 detection, viral load and infectivity over the course of an infection. *J. Infect.* **2020**, *81*, 357–371. [[CrossRef](#)]
6. Jones, D.; Baluja, M.Q.; Graham, D.W.; Corbishley, A.; McDonald, J.E.; Malham, S.K.; Hillary, L.S.; Connor, T.R.; Gaze, W.H.; Moura, I.B.; et al. Shedding of SARS-CoV-2 in faeces and urine and its potential role in person-to-person transmission and the environment-based spread of COVID-19. *Sci. Total Environ.* **2020**, *749*, 141364. [[CrossRef](#)]
7. Wu, Y.; Guo, C.; Tang, L.; Hong, Z.; Zhou, J.; Dong, X.; Yin, H.; Xiao, Q.; Tang, Y.; Qu, X.; et al. Prolonged presence of SARS-CoV-2 viral RNA in faecal samples. *Lancet Gastroenterol. Hepatol.* **2020**, *5*, 434–435. [[CrossRef](#)]
8. Xu, Y.; Li, X.; Zhu, B.; Liang, H.; Fang, C.; Gong, Y.; Guo, Q.; Sun, X.; Zhao, D.; Shen, J.; et al. Characteristics of pediatric SARS-CoV-2 infection and potential evidence for persistent fecal viral shedding. *Nat. Med.* **2020**, *26*, 502–505. [[CrossRef](#)]
9. Zuccato, E.; Chiabrando, C.; Castiglioni, S.; Calamari, D.; Bagnati, R.; Schiarea, S.; Fanelli, R. Cocaine in surface waters: A new evidence-based tool to monitor community drug abuse. *Environ. Health* **2005**, *4*, 14. [[CrossRef](#)]

10. Brouwer, A.F.; Eisenberg, J.; Pomeroy, C.D.; Shulman, L.M.; Hindiyeh, M.; Manor, Y.; Grotto, I.; Koopman, J.S.; Eisenberg, M.C. Epidemiology of the silent polio outbreak in Rahat, Israel, based on modeling of environmental surveillance data. *Proc. Natl. Acad. Sci. USA* **2018**, *115*, E10625–E10633. [CrossRef]
11. Iaconelli, M.; Ferraro, G.B.; Mancini, P.; Suffredini, E.; Veneri, C.; Ciccaglione, A.R.; Bruni, R.; Libera, S.D.; Bignami, F.; Brambilla, M.; et al. Nine-Year Nationwide Environmental Surveillance of Hepatitis E Virus in Urban Wastewaters in Italy (2011–2019). *Int. J. Environ. Res. Public Health* **2020**, *17*, 2059. [CrossRef]
12. Polo, D.; Quintela-Baluja, M.; Corbishley, A.; Jones, D.; Singer, A.; Graham, D.; Romalde, J. Making waves: Wastewater-based epidemiology for COVID-19—Approaches and challenges for surveillance and prediction. *Water Res.* **2020**, *186*, 116404. [CrossRef] [PubMed]
13. Thompson, J.N.; Gu, X.; Lee, E.; Rajal, V.; Haines, M.; Girones, R.; Ng, L.C.; Alm, E.J.; Wuertz, S. Makingwaves: Wastewater surveillance of SARS-CoV-2 for population-based health management. *Water Res.* **2020**, *184*, 116181. [CrossRef] [PubMed]
14. Hamouda, M.; Mustafa, F.; Maraqa, M.; Rizvi, T.; Hassan, A.A. Wastewater surveillance for SARS-CoV-2: Lessons learnt from recent studies to define future applications. *Sci. Total Environ.* **2021**, *759*, 143493. [CrossRef] [PubMed]
15. Lundy, L.; Fatta-Kassinos, D.; Solbodnik, J.; Karaolia, P.; Cirka, L.; Kreuzinger, N.; Castiglioni, S.; Bijlsma, L.; Dulio, V.; Deviller, G.; et al. Making Waves: Collaboration in the time of SARS-CoV-2—Rapid development of an international co-operation and wastewater surveillance database to support public health decision-making. *Water Res.* **2021**, *199*, 117167. [CrossRef] [PubMed]
16. Ahmed, W.; Bertsch, P.M.; Bibby, K.; Haramoto, E.; Hewitt, J.; Huygens, F.; Gyawali, P.; Korajkic, A.; Ridell, S.; Sherchan, S.P.; et al. Decay of SARS-CoV-2 and surrogate murine hepatitis virus RNA in untreated wastewater to inform application in wastewater-based epidemiology. *Environ. Res.* **2020**, *191*, 110092. [CrossRef] [PubMed]
17. Tran, J.N.; Gu, X.; Lee, E.; Rajal, V.; Haines, M.; Girones, R.; Ng, L.C.; Alm, E.J.; Wuertz, S. SARS-CoV-2 coronavirus in water and wastewater: A critical review about presence and concern. *Environ. Res.* **2021**, *193*, 110265. [CrossRef] [PubMed]
18. Wang, X.W.; Li, J.S.; Jin, M.; Zhen, B.; Kong, Q.X.; Song, N.; Xiao, W.J.; Chao, F.H.; Li, J.W. Study in the resistance of severe acute respiratory syndrome-associated coronavirus. *J. Virol. Methods* **2005**, *126*, 171–177. [CrossRef] [PubMed]
19. Wölfel, R.; Corman, V.M.; Guggemos, W.; Seilmaier, M.; Zange, S.; Mueller, M.A.; Niemeyer, D.; Vollmar, P.; Rothe, C.; Hoelscher, M.; et al. Virological assessment of hospitalized patients with COVID-19. *Nature* **2020**, *581*, 465–469. [CrossRef] [PubMed]
20. Muira, F.; Kitajima, M.; Omori, R. Duration of SARS-CoV-2 viral shedding in faeces as a parameter for wastewater-based epidemiology: Re-analysis of patient data using a shedding dynamics model. *Sci. Total Environ.* **2021**, *769*, 144549. [CrossRef] [PubMed]
21. Foladori, P.; Cutrupi, F.; Segata, N.; Manara, S.; Pinto, F.; Malpei, F.; Bruni, L.; Rosa, G. SARS-CoV-2 from faeces to wastewater treatment: What do we know? A review. *Sci. Total Environ.* **2020**, *743*, 140444. [CrossRef] [PubMed]
22. Medema, G.; Heijnen, L.; Elsinga, G.; Italiaander, R.; Brouwer, A. Presence of SARS-Coronavirus-2 RNA in Sewage and Correlation with Reported COVID-19 Prevalence in the Early Stage of the Epidemic in The Netherlands. *Environ. Sci. Technol. Lett.* **2020**, *7*, 511–516. [CrossRef]
23. D’Aoust, P.M.; Graber, T.E.; Mercier, E.; Montpetit, I.; Neault, N.; Baig, A.T.; Mayne, J.; Zhang, X.; Alin, T.; Servos, M.R.; et al. Catching a resurgence: Increase in SARS-CoV-2 viral RNA identified in wastewater 48 h before COVID-19 test and 96 h before hospitalizations. *Sci. Total Environ.* **2021**, *770*, 145319. [CrossRef] [PubMed]
24. Peccia, J.; Zulli, A.; Brackney, D.E.; Grubaugh, N.D.; Kaplan, E.H.; Casanovas-Massana, A.; Ko, A.I.; Malik, A.A.; Wang, D.; Wang, M.; et al. Measurement of SARS-CoV-2 RNA in wastewater tracks community infection dynamics. *Nat. Biotechnol.* **2020**, *38*, 1164–1167. [CrossRef] [PubMed]
25. Randazzo, W.; Truchado, P.; Cuevas-Ferrando, E.; Simón, P.; Allende, A.; Sánchez, G. SARS-CoV-2 RNA in wastewater anticipated COVID-19 occurrence in a low prevalence area. *Water Res.* **2020**, *181*, 115942. [CrossRef] [PubMed]
26. Been, F.; Rossi, L.; Ort, C.; Rudaz, A.; Delémont, O.; Esseiva, P. Population Normalization with Ammonium in Wastewater-Based Epidemiology: Application on Illicit Drug Monitoring. *Environ. Sci. Technol.* **2014**, *48*, 8162–8169. [CrossRef] [PubMed]
27. D’Aoust, P.M.; Mercier, E.; Montpetit, D.; Jia, J.J.; Alexandrov, I.; Neault, N.; Baig, A.T.; Mayne, J.; Zhang, X.; Alain, T.; et al. Quantitative analysis of SARS-CoV-2 RNA from wastewater solids in communities with low COVID-19 incidence and prevalence. *Water Res.* **2021**, *188*, 116560. [CrossRef] [PubMed]
28. O’Brien, J.W.; Thai, P.K.; Eaglesham, G.; Ort, C.; Scheidegger, A.; Carter, S.; Lai, F.Y.; Mueller, J.F. A Model to Estimate the Population Contributing to the Wastewater Using Samples Collected on Census Day. *Environ. Sci. Technol.* **2014**, *48*, 517–525. [CrossRef]
29. Norrbottens Klimat. Available online: <https://www.smhi.se/kunskapsbanken/klimat/klimatet-i-sveriges-landskap/norrbottens-klimat-1.5008> (accessed on 6 June 2021).
30. Dataserier Med Normalvärden för Perioden 1991–2020. Available online: <https://www.smhi.se/data/meteorologi/dataserier-med-normalvardnen-for-perioden-1991-2020-1.167775> (accessed on 28 April 2021).
31. Luleå Kommun. *Miljörapport Uddebo Avloppsreningsverk*; Version 2; Luleå Kommun: Luleå, Sweden, 2019.
32. Luleå Kommun. *Miljörapport Råneå Avloppsreningsverk*; Version 1; Luleå Kommun: Luleå, Sweden, 2019.
33. Nystedt, A. (Norrbotten County Council, Luleå, Sweden). Personal communication, 2021.
34. Mondal, S.; Feirer, N.; Brockman, M.; Preston, M.A.; Teter, S.J.; Ma, D.; Goueli, S.A.; Moorji, S.; Saul, B.; Cali, J.J. A direct capture method for purification and detection of viral nucleic acid enables epidemiological surveillance of SARS-CoV-2. *Sci. Total Environ.* **2021**, *795*, 148834. [CrossRef] [PubMed]

35. Vogels, C.B.F.; Brito, A.F.; Wyllie, A.L.; Fauver, J.R.; Ott, I.M.; Kalinich, C.C.; Petrone, M.E.; Casanovas-Massana, A.; Muenker, M.C.; Moore, A.J.; et al. Analytical sensitivity and efficiency comparisons of SARS-CoV-2 RT-qPCR primer-probe sets. *Nat. Microbiol.* **2020**, *5*, 1299–1305. [[CrossRef](#)]
36. Zhang, T.; Breitbart, M.; Lee, W.H.; Run, J.-Q.; Wie, C.L.; Soh, S.W.L.; Hibberd, M.L.; Liu, E.T.L.; Rohwer, F.; Ruan, Y. RNA viral community in human feces: Prevalence of plant pathogenic viruses. *PLoS Biol.* **2006**, *4*, 108–118. [[CrossRef](#)] [[PubMed](#)]
37. Bustin, S.A.; Benes, V.; Garson, J.A.; Hellems, J.; Huggett, J.; Kubista, M.; Mueller, R.; Nolan, T.; Pfaffl, M.W.; Shipley, G.L.; et al. The MIQE Guidelines: Minimum Information for Publication of Quantitative Real-Time PCR Experiments. *Clin. Chem.* **2009**, *55*, 611–622. [[CrossRef](#)] [[PubMed](#)]
38. Jönsson, H.; Baky, A.; Jeppsson, U.; Hellström, D.; Kärrman, E. *Composition of Urine, Faeces, Greywater and Biowaste for Utilization in the URWARE Model*; Report 2005:6; Chalmers University of Technology: Göteborg, Sweden, 2005.
39. Vinnerås, B.; Palmquist, H.; Balmér, P.; Jönsson, H. The characteristics of household wastewater and biodegradable solid waste—A proposal for new Swedish design values. *Urban Water J.* **2006**, *3*, 3–11. [[CrossRef](#)]
40. Van Nuijs, A.; Mougel, J.-F.; Tarcomnicu, I.; Bervoets, L.; Blust, R.; Jorens, P.G.; Neels, H.; Covaci, A. Sewage epidemiology—A real-time approach to estimate the consumption of illicit drugs in Brussels, Belgium. *Environ. Int.* **2011**, *37*, 612–621. [[CrossRef](#)] [[PubMed](#)]
41. Press, C.; Davidsson, F.; Wellsjö, L.; Grubbström, E.; Ridelius, A. Hushållspillvattenundersökning. Report 2019:5, Gryaab. Available online: <https://www.gryaab.se/om-gryaab/publikationer-och-informationsmaterial/> (accessed on 18 August 2021).
42. Zheng, Q.D.; Wang, Z.; Liu, C.Y.; Yan, J.H.; Pei, W.; Wang, Z.; Wang, D.G. Applying a population model based on hydrochemical parameters in wastewater-based epidemiology. *Sci. Total Environ.* **2019**, *657*, 466–475. [[CrossRef](#)] [[PubMed](#)]
43. Rico, M.; Andrés-Costa, M.J.; Picó, Y. Estimating population size in wastewater-based epidemiology. Valencia metropolitan area as a case study. *J. Hazard Mater.* **2017**, *323*, 156–165. [[CrossRef](#)] [[PubMed](#)]
44. Pandopoulos, A.J.; Bade, R.; Tschärke, B.J.; O’Brian, J.W.; Simpson, B.S.; White, J.M.; Gerber, C. Application of catecholamine metabolites as endogenous population biomarkers for wastewater-based epidemiology. *Sci. Total Environ.* **2021**, *763*, 142992. [[CrossRef](#)] [[PubMed](#)]
45. Choi, P.M.; Tschärke, B.J.; Donner, E.; O’Brian, J.W.; Grant, S.C.; Kaserzon, S.L.; Mackie, R.; O’Malley, E.; Crosbie, N.D.; Thomas, K.V.; et al. Wastewater-based epidemiology biomarker: Past, present and future. *Trends Anal. Chem.* **2018**, *105*, 453–469. [[CrossRef](#)]
46. Lai, F.; Anuj, S.; Bruna, R.; Carter, S.; Gartner, C.; Hall, W.; Kirkbride, K.P.; Mueller, J.F.; O’Brian, J.W.; Prichard, J.; et al. Systematic and day-to-day effects of chemical-derived population estimates on wastewater-based drug epidemiology. *Environ. Sci. Technol.* **2015**, *49*, 999–1008. [[CrossRef](#)] [[PubMed](#)]
47. Symonds, E.M.; Rosario, K.; Breitbart, M. Pepper mild mottle virus: Agricultural menace turned effective tool for microbial water quality monitoring and assessing (waste) water treatment technologies. *PLoS Pathog.* **2019**, *15*, e0208552. [[CrossRef](#)]
48. Kitajima, M.; Sassi, H.P.; Torrey, J.R. Pepper mild mottle virus as a water quality indicator. *Npj Clean Water* **2018**, *1*, 19. [[CrossRef](#)]
49. Jafferli, M.H.; Khatami, K.; Atasoy, M.; Birgersson, M.; Williams, C.; Cetecioglu, Z. Benchmarking virus concentrations methods for quantification of SARS-CoV-2 in raw wastewater. *Sci. Total Environ.* **2021**, *755*, 142939. [[CrossRef](#)] [[PubMed](#)]